

1 **18-crown-6-sodium cholate complex: thermochemistry, structure and**  
2 **stability**

3 Tea Mihelj<sup>1\*</sup>, Vlasta Tomašić<sup>1\*</sup>, Nikola Biliškov<sup>2</sup>

4 <sup>1</sup>*Department of Physical Chemistry, Ruđer Bošković Institute, POB 180, HR-10002 Zagreb,*  
5 *Croatia*

6 <sup>2</sup>*Division of Materials Chemistry, Ruđer Bošković Institute, POB 180, HR-10002 Zagreb,*  
7 *Croatia*

8  
9  
10 <sup>\*</sup>To whom correspondence should be addressed:

11 Email: [tmihelj@irb.hr](mailto:tmihelj@irb.hr), [vlastom@irb.hr](mailto:vlastom@irb.hr)

12  
13 Ruđer Bošković Institute, Department of Physical Chemistry

14 [Laboratory for synthesis and processes of self-assembling of organic molecules](#)

15 Bijenička c. 54, P.O. Box 180, HR-10002 Zagreb, Croatia

16 Fax: +38514680245

17 Tel: +38514571211

18

19

20

21

22

23

1           **Abstract**

2           18-crown-6, one of the most relevant crown ethers, and sodium cholate, steroidal surfactant  
3           classified as natural bile salt, are components of novel, synthesized coordination complex; 18-crown-  
4           6-sodium cholate (18C6·NaCh). Like crown ethers, bile salts act as building blocks in supramolecular  
5           chemistry in order to design new functionalized materials with a desired structure and properties. In  
6           order to obtain thermal behavior of this 1:1 coordination complex, thermogravimetry and differential  
7           thermal analysis were used, as well as microscopic observations and differential scanning calorimetry.  
8           Temperature dependent infrared spectroscopy (IR) gave a detailed view into phase transitions. The  
9           structures during thermal treatment were observed with powder X-ray diffraction, and molecular  
10          models of the phases are made.

11          Hard, glassy, colorless compound 18C6·NaCh goes through crystalline – crystalline  
12          polymorphic phase transitions at higher temperatures. The room temperature phase is indexed to a  
13          triclinic lattice, while in the high temperature phases molecules take randomly one of the two different  
14          configurations in the unit cell, resulting in the 2-fold symmetry. The formation of cholesteric liquid  
15          crystalline phase occurs simultaneously with partial decomposition, followed by the isotropisation  
16          with simultaneous and complete decomposition at much higher temperature, as obtained by IR. The  
17          results provide valuable information about the relationship between molecular structure, thermal  
18          properties, and stability of the complex, indicating the importance of an appropriate choice of cation,  
19          amphiphilic, and crown ether unit in order to synthesize compounds with desired behavior.

20  
21  
22  
23  
24  
25  
26

1 **Keywords:** 18-crown-6, sodium cholate, structure, NMR, thermal behavior, IR spectroscopy

2

3

4

5

6

7

8

9

10

11

12

13

14

15

16

17

18

19

20

21

22

## 1 1. INTRODUCTION

2 Crown ethers constitute one of the most prominent molecules in host-guest chemistry, often  
3 called the simplest bench-mark substrates resembling the general features of key-pocket inclusion  
4 complexes.<sup>1</sup> Among most salient properties of crown ethers stands their specific binding and solvation  
5 of cationic species; alkali, alkaline-earth, transition-metal, and ammonium cations,<sup>2-6</sup> which makes  
6 them a perfect and valuable tool in organic synthesis. These macrocyclic polyethers are known as  
7 neutral complexing agents, with specific selectivity as the result of their cavity size that adopts cations  
8 of comparable ionic radii and the capability of the cyclic ether backbone to build a coordination shell,  
9 optimizing the interaction of its electron donor oxygen sites with the cation.<sup>7-9</sup> The number, and type  
10 of donor atoms, conformational flexibility for most effective coordination, as well as the size and form  
11 of the coordinated guest and charge density dictate different binding activity, as well as  
12 preorganization by means of symmetric and chiral arrangements and the solvent effect.<sup>4,8,10,11</sup>  
13 Consequently, these “ionophore-model systems” are very attractive to chemists and applicable in  
14 many areas; from biological mimics, and models of biological receptors,<sup>12</sup> to recovery, removal or  
15 selective complexation and transport of species,<sup>13</sup> usage in environmental,<sup>14,15</sup> as well as  
16 pharmaceutical<sup>16,17</sup> applications. Moreover, they have been used as building blocks for a broad range  
17 of modern materials<sup>10,18,19</sup> chromatographic agents<sup>20,21</sup> *etc.* Alkali metal elements have important role  
18 in biological processes, primarily as bulk electrolytes that stabilize surface charges on proteins and  
19 nucleic acids,<sup>22</sup> and also play unique structural role in biological systems.<sup>23,24</sup> Crown-ligands with  
20 alkali metal elements make coordination compounds based on electrostatic interaction through ion-  
21 dipole attractions,<sup>25</sup> useful for simulations of properties and behavior of natural substances.

22 Cholic acid is a steroidal surfactant compound classified as a natural bile acid. The literature  
23 describes a vast amount of pharmacological applications of bile acids and their derivatives, including the  
24 use in treatment of their deficiency, dissolution of cholesterol gallstones,<sup>26</sup> antiviral<sup>27</sup> and antifungal  
25 properties.<sup>28</sup> Like crown ethers, bile acids act as building blocks in supramolecular chemistry in order  
26 to design new antibiotics,<sup>29</sup> cationic or anionic receptors,<sup>30,31</sup> templates, scaffolds or ionic channels.<sup>32,33</sup>  
27 Some of cholic acid based macrocyclic compounds are cholaphanes usually used as transmembrane

1 anion carriers,<sup>34</sup> cyclocholates used in host-guest chemistry or molecular recognition studies<sup>35</sup>, as well  
2 as bile acid based chiral dendrons of nanometric dimensions<sup>36</sup>, or molecular boxes.<sup>37</sup> It is already  
3 known that cholic acid forms inclusion crystals with various guest compounds.

4 Attempts to form inclusion crystals of cholic acid with various guest compounds have  
5 revealed a variety of molecular assemblies, with the hydrogen bonding directly involved in the  
6 structure of bile acid crystals and forming different network patterns; from two-dimensional sheets<sup>38,39</sup>  
7 to three-dimensional host framework, making cumulated channel-type bilayers, accompanied with  
8 guest responsive transformations of crystal structure, and variable guest-dependent polymorphism.<sup>40,41</sup>  
9 Host-guest compounds of cholic acid with *n*-alkylammonia revealed two types of bilayer like  
10 structures; in 1:1 complexes guests are included in the hydrophobic zones between those layers in a  
11 kind of sandwich-type structure, while in 2:1 compound bilayers cross and form one-dimensional  
12 hydrophobic channels into which guest molecules are included.<sup>42</sup> Besides crossing structures with  
13 cage-like cavities and bilayered structures with channel-like cavities, the honeycomb structure with  
14 hexagonal channels is also representative crystal structure of cholic acid derivatives.<sup>43</sup> In general, more  
15 than thirteen kinds of host frameworks, differing in volume, shape, polarity and chirality of guests  
16 have been found so far.<sup>38,39</sup> Diversity is the result of the hierarchical structure in steroids, based on  
17 characteristic bimolecular and helical  $2_1$  screw assemblies,<sup>44</sup> retained by the hydrogen bonding  
18 network of the three hydroxyl groups in the steroidal skeleton, and building bundles. Moreover, it is  
19 the result of the steroidal skeleton asymmetry, facial amphiphilicity of molecules,<sup>40</sup> type of guest  
20 components,<sup>42</sup> and various combination of hydrogen-bonding arrangements. In principle, the bile salt  
21 molecules possess information, expressed through their molecular architecture.

22 Complexes formed between crown ether compounds and surfactants are less explored,  
23 especially in terms of thermochemical studies. A lot of studies made on crown ether complexes  
24 informed about thermotropic mesomorphism during thermal treatment; from hexagonal columnar  
25 mesophases in complexes with 18-crown-6 derivatives,<sup>45,46</sup> to cholesteric liquid crystalline behavior for  
26 cholesteryl esters bearing 16-membered crown ethers.<sup>47</sup> Complexes with crown ethers containing aza,  
27 thio units or other heteroatoms have also shown rich thermal behavior with polymorphism and liquid

1 crystal formation.<sup>48-51</sup> This manuscript comprises structural and thermochemical study of novel 18-  
2 crown-6 (18C6) complex with sodium cholate. X-ray diffraction techniques are one of the most  
3 reliable methods to solve the structure. Due to complex nature of steroidal compounds and thus more  
4 tedious procedure, single X-ray diffraction has been more often used in determination of molecular  
5 arrangement in crystals,<sup>39,42,52-54</sup> rather than powder X-ray diffraction. In this study structure of 18C6-  
6 sodium cholate complex is completely characterized with temperature dependent powder X-ray  
7 diffraction technique. Besides thermogravimetry, microscopic observations and differential scanning  
8 calorimetry, infrared spectroscopy in a wide temperature range was used. It was recently shown by  
9 Zimmermann and Baranović<sup>55</sup> that phase transitions can be detected by rapid and simple analysis of  
10 absolute variations of a baseline in a temperature-dependent mid-infrared transmittance spectra. The  
11 method is based exclusively on changes in optical properties of the material under investigation. Thus,  
12 some phase transitions, overlooked by more commonly used methods, become readily evident by IR  
13 spectroscopy, as seen in our recent publications.<sup>56,57</sup> Further advantage of temperature-dependent IR  
14 spectroscopy lies in the fact that it provides an elegant link between macroscopic and microscopic  
15 properties. In other words, it does not only detect phase transitions, but the variations in the fingerprint  
16 region of the recorded spectra reflect the changes at molecular level, which are manifested at  
17 macroscopic level as phase transitions. The results given in this study provide valuable information  
18 about the relationship between molecular structure, thermal properties, and stability of the complex,  
19 indicating the importance of an appropriate choice of cation and crown ether unit in order to  
20 synthesize compounds with eligible behavior. Such experiments widen the research field of ion  
21 complexation and supramolecular chemistry in order to make new, functionalized materials with a  
22 desired structure and properties.

23

24

25

26

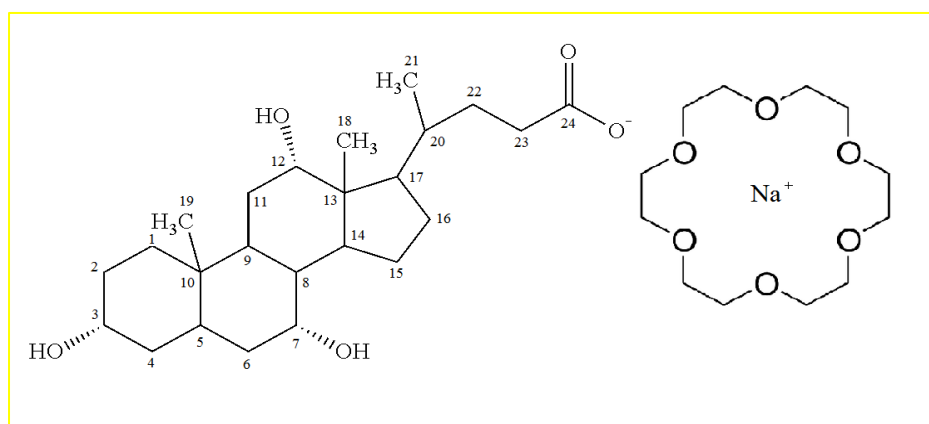
## 1 2. EXPERIMENTAL

### 2 Materials, complex preparation and identification

3 18-crown-6 ether, *i.e.* 1,4,7,10,13,16-hexaoxacyclooctadecane (18C6,  $C_{12}H_{24}O_6$ ,  $M_w = 264.32$   
4  $g\ mol^{-1}$ ) and sodium cholate hydrate, *i.e.* 3 $\alpha$ ,7 $\alpha$ ,12 $\alpha$ -trihydroxy-5 $\beta$ -cholanic-acid sodium salt (NaCh,  
5  $C_{24}H_{39}O_5Na$ ,  $M_w/g\ mol^{-1} = 430.60\ g\ mol^{-1}$ ; Sigma Ultra, min. 99%) were obtained from Sigma Aldrich  
6 and used without further purification for the preparation of the complex.

7 18-Crown-6- sodium cholate complex (18C6·NaCh) was prepared by high temperature mixing  
8 of equimolar aqueous solutions of both components. After aging (few days at room temperature)  
9 during which water spontaneously evaporated, the sample was dried under vacuum at room  
10 temperature (RT) until constant mass was obtained, and stored protected from moisture and light  
11 before use. Such precipitated compound was waxy and after vacuum dried, glassy, colorless and  
12 transparent.

13 The identification of complex was performed by *elemental analysis* (Perkin-Elmer Analyzer  
14 PE 2400 Series 2). Elemental analysis expressed as mass fraction in percent confirmed that the  
15 complex is 1:1 charge ratio adduct;  $C_{36}H_{63}O_{11}Na$ ,  $M_w = 694.92\ g\ mol^{-1}$ . Found: C, 62.30; H, 9.20;  
16 requires C, 62.23; H, 9.14 %. It was also characterized by *nuclear magnetic resonance spectroscopy*,  
17 NMR (Avance 600 Bruker with supraconducting magnet, 14 T field strength, frequency range 24-600  
18 MHz and temperature range 223-373 K) according to the following designation:



1  $^{13}\text{C}$  NMR (150 MHz,  $\text{D}_2\text{O}$ , 323.15 K)  $\sigma$ /ppm: 73.45 (C12), 71.91 (C3), 69.85 ( $\text{CH}_2$  (crown)),  
2 68.62 (C7), 47.03 (C17), 46.48 (C13), 41.85 (C5), 41.48 (C14), 39.61 (C8), 38.82 (C4), 35.72 (C20),  
3 35.17 (C23), 34.67 (C10), 34.21 (C6), 32.52 (C22), 29.65 (C2), 28.02 (C11), 27.48 (C16), 26.73 (C9),  
4 23.21 (C15), 22.38 (C19), 17.14 (C21), 12.42 (C18).

5  $^1\text{H}$  NMR (600 MHz,  $\text{D}_2\text{O}$ , 323.15 K)  $\sigma$ /ppm; 4.76 (1H, s, OH (C3)), 4.34 (1H, s br, OH  
6 (C12)), 4.18 (1H, s br, OH (C7)), 4.12-3.96 (24H, s,  $\text{CH}_2$  (crown)), 3.96 (1H, s, CH (C7)), 3.81-3.75  
7 (1H, m,  $J = 4.137$  CH (C3)), 2.55 (1H, m,  $\text{CH}_2$  (C23)), 2.47-2.34 (3H, m,  $\text{CH}_2$  (C4, C23), CH (C9)),  
8 2.29-2.21 (2H, m,  $\text{CH}_2$  (C22, C6)), 2.17-2.09 (2H, m,  $\text{CH}_2$  (C4), CH (C14)), 2.06-1.84 (10 H, m,  $\text{CH}_2$   
9 (C22, C1, C15, C2, C11, C6, C16), CH (C17, C8)), 1.74-1.58 (5H, m,  $\text{CH}_2$  (C2, C16), CH (C20, C5)),  
10 1.29 (3H, d,  $J = 6.44$ ,  $\text{CH}_3$  (C21)), 1.21 (3H, s,  $\text{CH}_3$  (C19)), 1.01(3H, s,  $\text{CH}_3$  (C18)).

11

## 12 **Measurements**

13 The loss of weight due to the heating was measured by *thermogravimetry*, TG, with an  
14 instrument Shimatzu DTG-60H. Sample was heated from RT to 573 K at the heating rate of 5 K  $\text{min}^{-1}$   
15 in synthetic airflow of 50 mL  $\text{min}^{-1}$ . The temperature range for thermal analysis of the sample was  
16 determined by examination of TG and DTA (differential thermal analysis) curves.

17 *Differential scanning calorimetry*, DSC, was carried out with a Perkin Elmer Pyris Diamond  
18 DSC calorimeter in  $\text{N}_2$  atmosphere equipped with a model Perkin Elmer 2P intra-cooler in  $\text{N}_2$   
19 atmosphere, at the rate of 2 K  $\text{min}^{-1}$ . Temperature and enthalpy calibrations were performed using high  
20 purity standard (*n*-decane and indium). The transition enthalpy,  $\Delta H/\text{kJ mol}^{-1}$ , was determined from the  
21 peak area of the DSC thermogram; and the corresponding entropy change,  $\Delta S/\text{J mol}^{-1} \text{K}^{-1}$ , was  
22 calculated using the maximal transition temperature. All results are mean values of several  
23 independent measurements carried out on different samples of the same compound, taken from the  
24 first heating and cooling run.

25 *Textures* were examined with Leica DMLS polarized optical light microscope, equipped with  
26 a Mettler FP 82 hot stage, Sony digital color video camera (SSC-DC58AP).



1            *Infrared transmission spectra* of the solid samples were recorded at 4 cm<sup>-1</sup> resolution in KBr  
2 pellets on an ABB Bomem MB102 single-beam FT-IR spectrometer with CsI optics, DTGS detector.  
3 The KBr sample pellets were prepared by mixing ~2 mg of the individual sample with 100 mg of KBr  
4 with a pestle and mortar made of agate. The use of KBr as matrix allows the usable spectral range of  
5 4000–300 cm<sup>-1</sup>. Each spectrum represents an average of 100 Fourier-transformed interferograms.  
6 Specac 3000 Series high-stability temperature controller with water cooled heating jacket was used to  
7 measure the spectra within the temperature range from RT up to 523 K under atmospheric conditions  
8 and at heating rate of 2 K min<sup>-1</sup> and 2 K steps. In variable-temperature infrared spectroscopy, heat is  
9 used as an outside perturbation, while the consequent changes in infrared spectra reflect the  
10 rearrangement of the sample on molecular level. It should be remarked that experimental setup, *i.e.*  
11 KBr pellets transmission technique, constitutes a thermodynamically open system. Thus, it allows free  
12 diffusion of the gaseous products, which arise due to the heating of the sample. Each single-beam  
13 spectrum collected in a temperature run for individual sample was ratioed to the single-beam spectrum  
14 of the sample-free setup (the reference spectrum) recorded immediately before starting the  
15 temperature-dependent measurements.

16            The *powder X-ray (PXRD) diffractograms* were recorded using a rotating anode copper source  
17 ( $\lambda/\text{\AA} = 1.54$ ) and a MAR345 image plate detector. The powder sample was put in a glass capillary,  
18 and its temperature was controlled using a cryojet system (Oxford Instrument). The 2-d diffraction  
19 patterns were converted to  $I-2\theta$  curves by radial average.

20

## 21 **Thermodynamics of the 18C6-crown decomplexation**

22            Thermodynamics of the 18C6-crown decomplexation process was considered by infrared  
23 spectroscopy. Since decomplexed 18C6 crown is free to diffuse from the system, decomplexation is  
24 determined by equilibrium constant defined as:  $K = \frac{[\text{MA}]}{[\text{18C6-MA}]}$  (1),  
25 where the 18C6-MA and MA state for complexed and decomplexed salt of M = sodium (Na) and  
26 anion A = cholate (Ch), respectively. The amount of the produced MA is given by:

1  $[MA] = c_0 (18C6 - MA) - [18C6 - MA]$  (2).

2 Since the experimental conditions allow free diffusion of the decomplexed 18C6 crown from  
3 the system, the expression for equilibrium constant is simplified to (3):

4 
$$K = \frac{c_0 (18C6-MA) - [18C6-MA]}{[18C6-MA]}$$
 (3).

5 Obviously, at room temperature  $[18C6 - MA] = c_0 (18C6 - MA)$ , while at the end of  
6 decomplexation  $[18C6 - MA] = 0 \text{ mol dm}^{-3}$ . In terms of spectroscopic observables, the equilibrium

7 constant is: 
$$K = \frac{A_0 (18C6-MA)}{A(18C6-MA)} - 1$$
 (4),

8 where  $A_0 (18C6 - MA)$  is absorbance of the band due to the 18C6-MA complex at 353 K, *i.e.* when  
9 sample is dehydrated. Now, combining the expression for equilibrium constant (4) with general  
10 expression for temperature dependence of equilibrium constant (5):

11 
$$\ln K(T) = -\frac{\Delta H}{kT} + \frac{\Delta S}{k}$$
 (5),

12 we obtain (6): 
$$\ln \left[ \frac{A_0 (18C6-MA)}{A(18C6-MA)} - 1 \right] = -\frac{\Delta H}{kT} + \frac{\Delta S}{k}$$
 (6).

13 Therefore, enthalpy and entropy changes due to the decomplexation are readily obtained from the  
14 absorbance measurement of complexed and decomplexed sodium salt.

15

16 **Table 1.** Transition temperatures,  $T/K$ , enthalpies,  $\Delta H/kJ \text{ mol}^{-1}$ , and entropies,  $\Delta S/J \text{ mol}^{-1} \text{ K}^{-1}$ , during  
17 heating and cooling cycles given by DSC measurements for 18C6·NaCh complex, together with the  
18 parameters for irreversible decomplexation (superscript d) of crown 18C6 from synthesized  
19 compound, calculated from the absorbance measurement of complexed and decomplexed sodium salt.

<b>Heating</b>		
$T/K$	$\Delta H/kJ \text{ mol}^{-1}$	$\Delta S/J \text{ mol}^{-1} \text{ K}^{-1}$
346.8	27.0	77.9
380.6	2.4	6.2
410.2	0.5	1.2

---

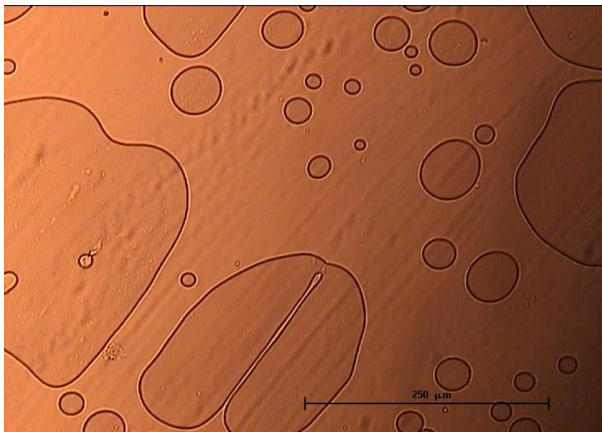
445.0 <sup>d</sup>	65.3	160.4
--------------------	------	-------

---

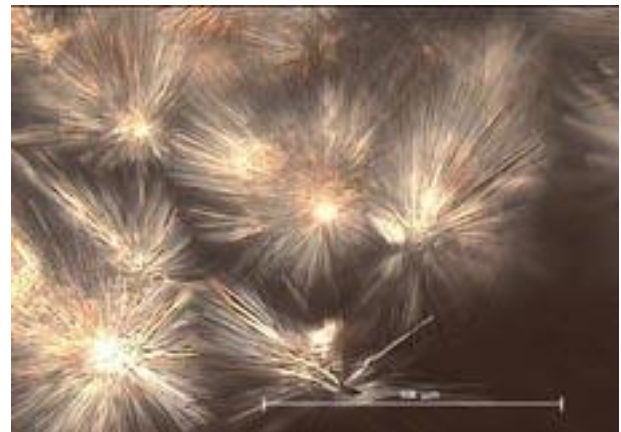
1

2

3 **Figure 1.** The micrographs of the characteristic textures for examined complex taken in the heating  
4 cycle by the optical microscope, under phase contrast (a) and crossed polarizers (b - d): RT (a); 355 K  
5 (b); 386 K (c), 400 K (d). The bar represents 250  $\mu\text{m}$  (a and c) and 100  $\mu\text{m}$  (b and d).



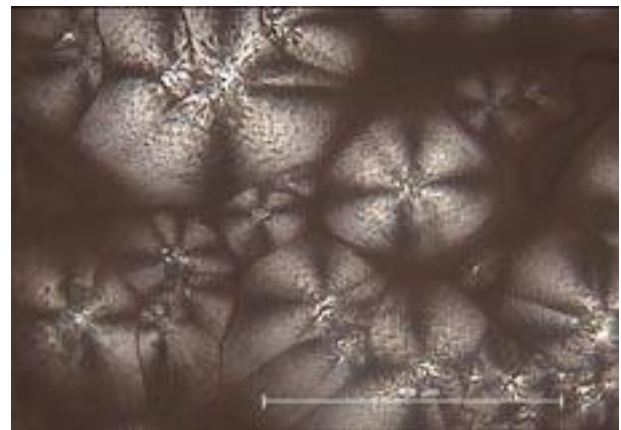
**a**



**b**



**c**



**d**

6

7

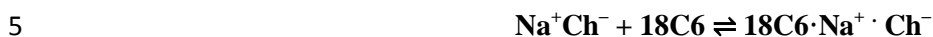
8

9

### 1 3. RESULTS AND DISCUSSION

#### 2 Solid-state phase transitions

3 Formation of solid 1:1 complex 18-crown-6-sodium cholate (18C6·NaCh) is accomplished  
4 through the equilibrium defined as:

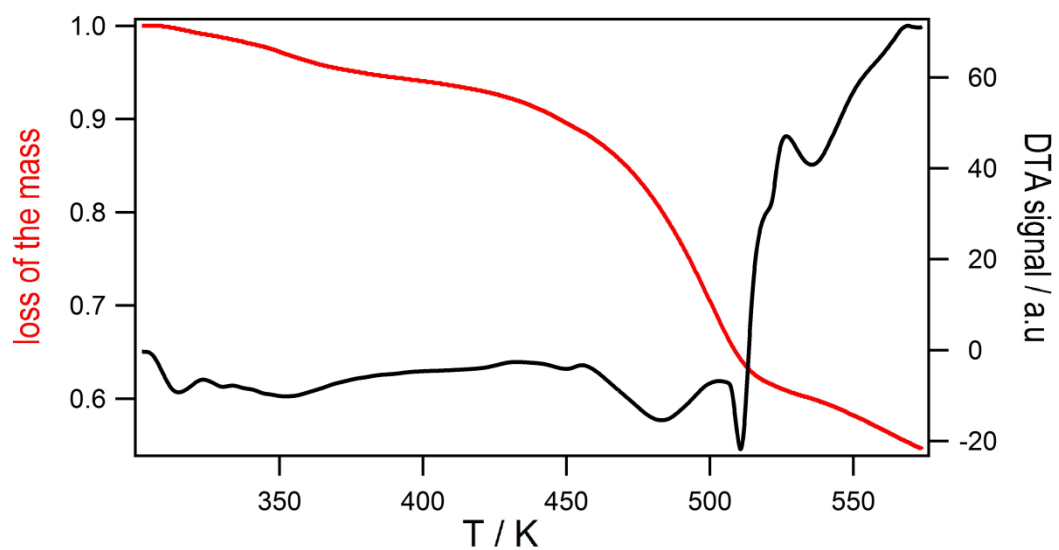


6 It is hard, glassy, colorless and transparent compound (Figure 1a), which becomes crystalline by  
7 complete dehydration (Figure 1b) at *cca.* 355 K, as evident from TG, DSC and temperature-dependent  
8 IR spectroscopy (Figures 2a and b, Figure 3a and c). TG shows that the water contributes by 5 % in  
9 the mass of the sample, which means that 2 water molecules bind to every 18C6·NaCh molecule. A  
10 prominent DSC endothermic peak (Table 1) indicates moderate O-H···O type hydrogen bonding. The  
11 most important functional groups assigned to spectral features at room temperature (RT) are presented  
12 in Figure 3a and Table 2. A slight rise of infrared baseline absorption at 353 K is well correlated with  
13 decrease of the mass, as observed by TG. Thus, it indicates dehydration of the sample. In this  
14 temperature region, IR spectra suffer the most prominent change in the 3700-3180 cm<sup>-1</sup> range,  
15 attributed to hydrogen bonded water symmetric and antisymmetric OH stretching oscillators, but also  
16 to OH groups of cholate anion. Thus, this region was considered in more details, and is explained in  
17 Supporting Information (Figure S1). Comparison with TG and DSC data shows that dehydration  
18 occurs as two-step process, of which the first ends at 360 K. This corresponds well to behavior of the  
19 features due to the 18C6 moiety (Figure 4a and b). The step of dehydration is mainly due to water  
20 which is hydrogen bonded to 18C6 crown moiety. This explains the steep decrease of the intensity of  
21 the bands corresponding to characteristic ether ν(C-O-C) band at 964 cm<sup>-1</sup> (Figure 4b), caused by the  
22 decrease in electron density on oxygen atoms of 18C6.

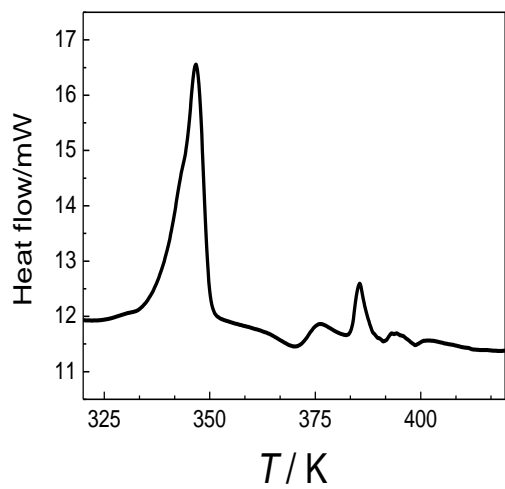
23

24 **Figure 2.** Representative thermogram (red line) and DTA result (black line) (a); DSC thermogram (b)  
25 for examined complex 18C6·NaCh; and thermodynamics of crown 18C6 decomplexation from

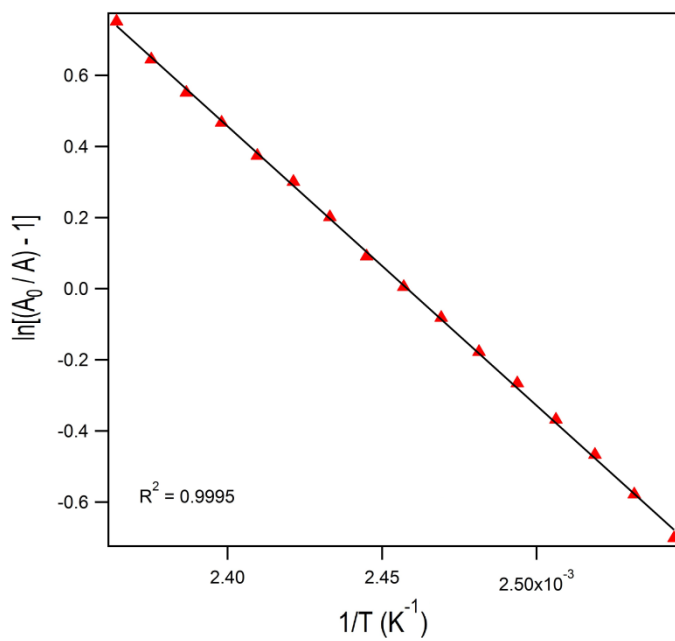
- 1 18C6·NaCh complex given by the IR (c). The PXRD diffractograms of 18C6·NaCh at different
- 2 temperatures, chosen and indexed due to obtained thermal changes at characteristic temperatures (d).



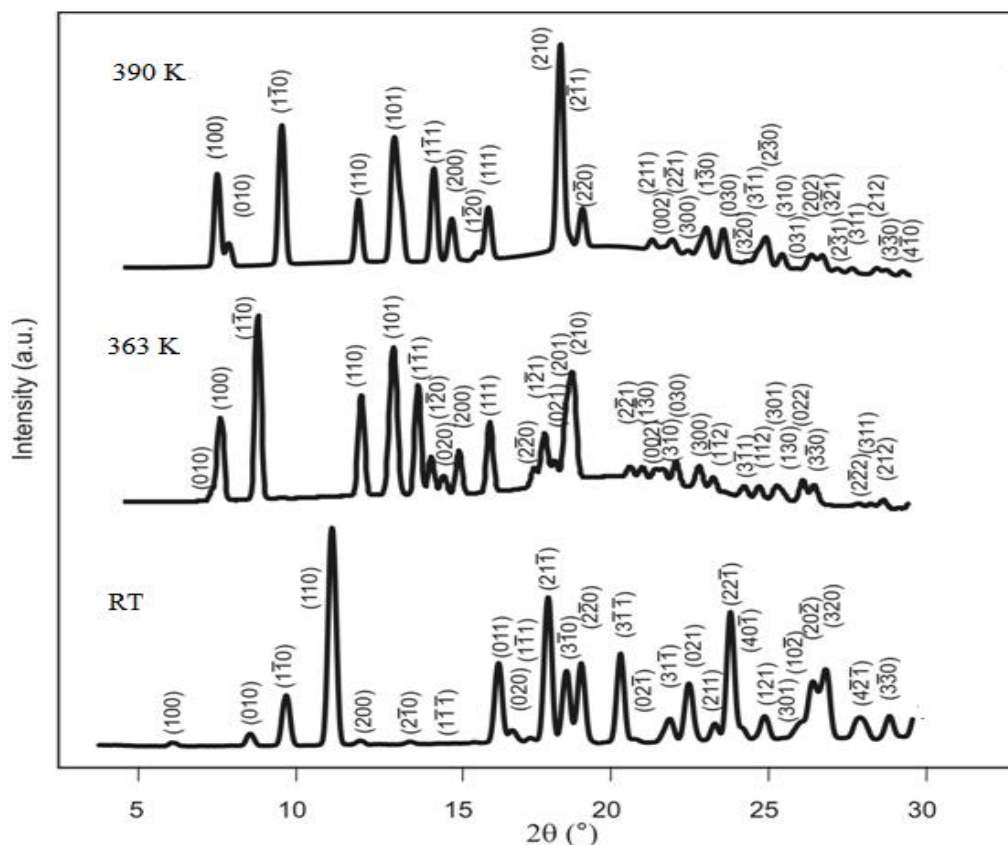
**a**



**b**



**c**



d

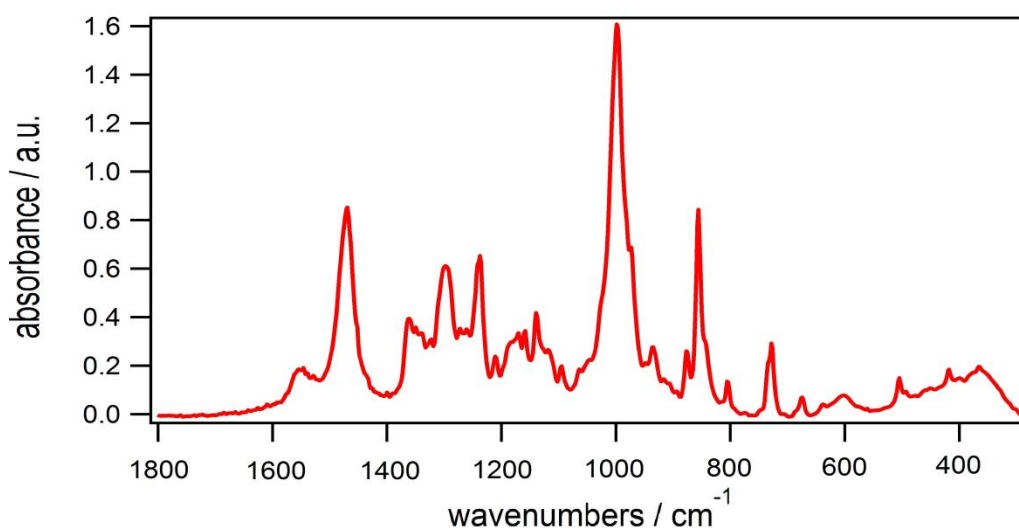
1  
2 After that, another step occurs between 370 and 390 K, simultaneously with changes of cholate  
3 symmetric  $\nu(\text{COO})$  band (Figure 4c and e), together with only a moderate decrease of intensity of the  
4  $18\text{C}6$  bands at  $964\text{ cm}^{-1}$  and  $1107\text{ cm}^{-1}$  (Figure 4a and 4b). This is in accordance with the DSC result  
5 of obtained polymorphic phase transition at 380 K (Table 1 and Figure 1c). A sudden shift toward the  
6 lower wavenumbers of both antisymmetric and symmetric  $\nu(\text{COO})$  bands is observed around 380 K.  
7 This is accompanied by increase of the intensity of antisymmetric band (Figure 4d) and moderate  
8 decrease of the symmetric band intensity (Figure 4e). The observations show that one of the water  
9 molecules is hydrogen-bonded to  $18\text{C}6$  moiety, while another is in slightly stronger interaction with  
10 carboxylic group of cholate anion. Increase of  $\nu_{\text{as}}(\text{COO})$  band intensity indicates an increasing ionic  
11 character of the bonding between  $\text{Na}^+$  and carboxylate moiety of cholate, caused by release of  
12 hydrogen bonded water molecule. Difference of the  $\nu_{\text{as}}(\text{COO})$  and  $\nu_{\text{s}}(\text{COO})$  band positions indicate  
13 monodentate bonding over the whole temperature range. The most significant change occurs around

1 380 K, when for the symmetric band shift of  $\Delta\nu_s = 15 \text{ cm}^{-1}$  is observed, while for antisymmetric band  
2 no shift is resolved in the spectra. This gives the change in mutual distance between antisymmetric and  
3 symmetric band from 172 to 185  $\text{cm}^{-1}$ . This transition obviously corresponds to change in bonding due  
4 to the dehydration and partial decomplexation of 18C6. However, TG does not show a significant  
5 decrease of the mass, which indicates that decomplexed 18C6 mainly remains in the sample.  
6 Decomplexation of 18C6 from NaCh·18C6 is also confirmed by comparison of IR spectra of the  
7 sample as obtained above 400 K with spectrum of purchased NaCh (see Supplementary data, Figure  
8 S2).

9  
10

11 **Figure 3.** Infrared spectra of 18C6·NaCh complex at room temperature in the 1900-400  $\text{cm}^{-1}$  region  
12 (a). Baseline corrected variable-temperature infrared spectra in the 323-473 K temperature interval (b),  
13 and temperature dependence of the baseline absorption (c). Inset shows the first derivative of the curve  
14 for the purposes of determination of the transition temperature. The detailed view of spectra with the  
15 most prominent changes at defined temperatures is seen in Figure S1 (Supplementary material).

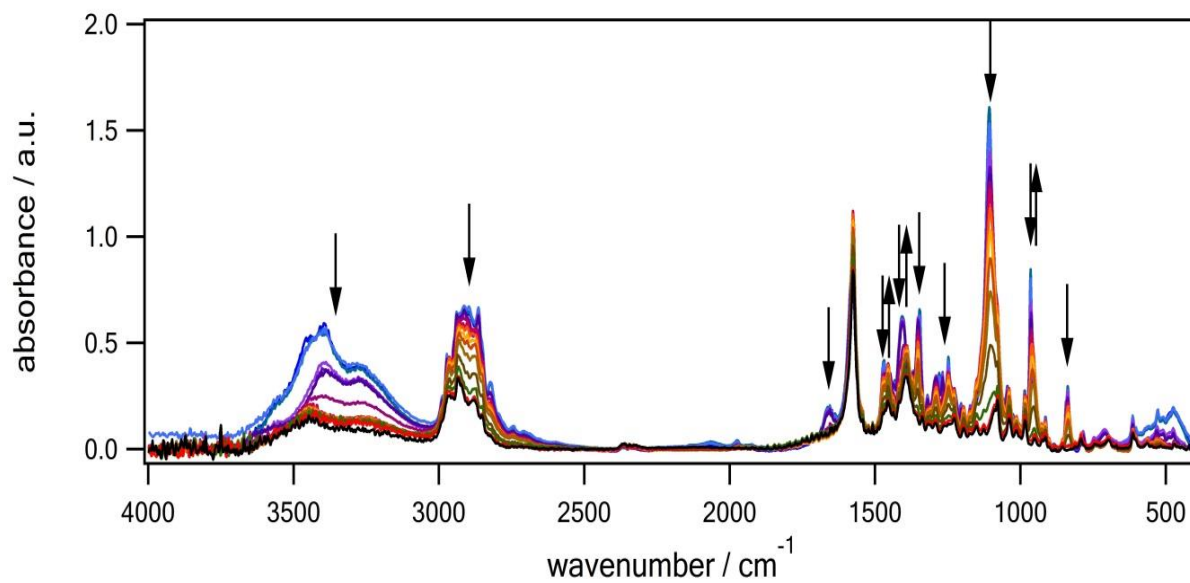
16



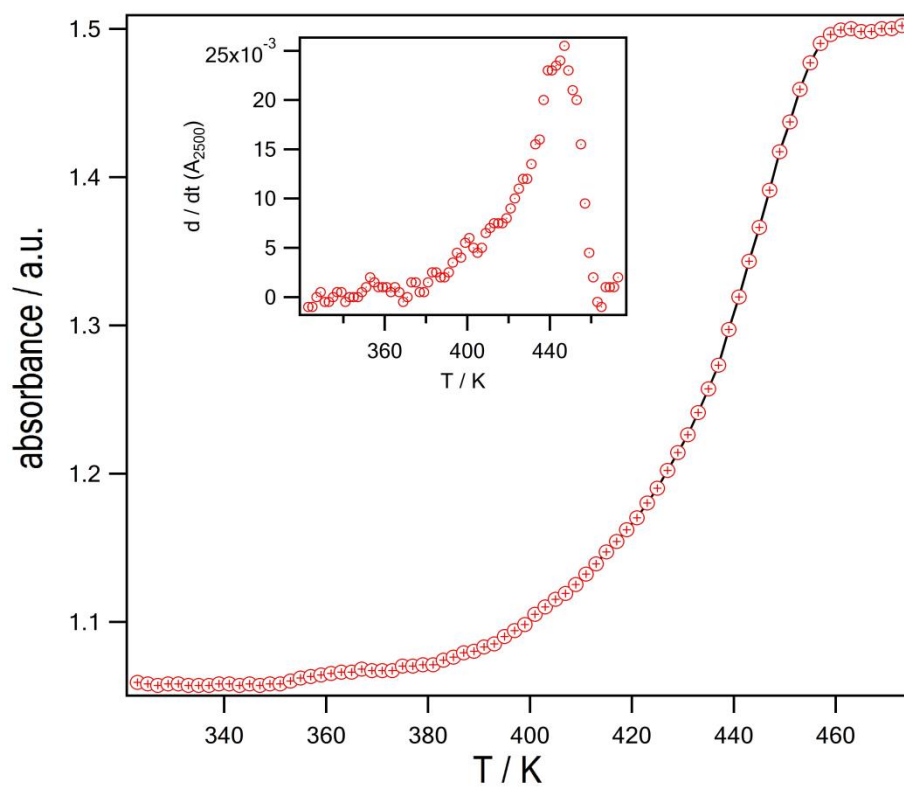
17

18

**a**



**b**



**c**

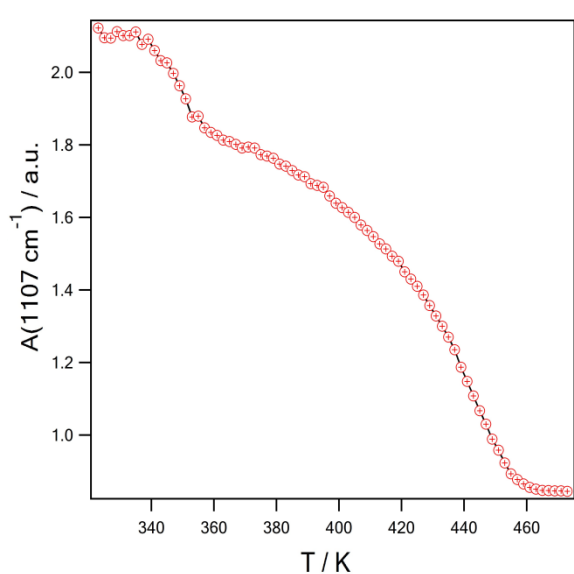
1

2

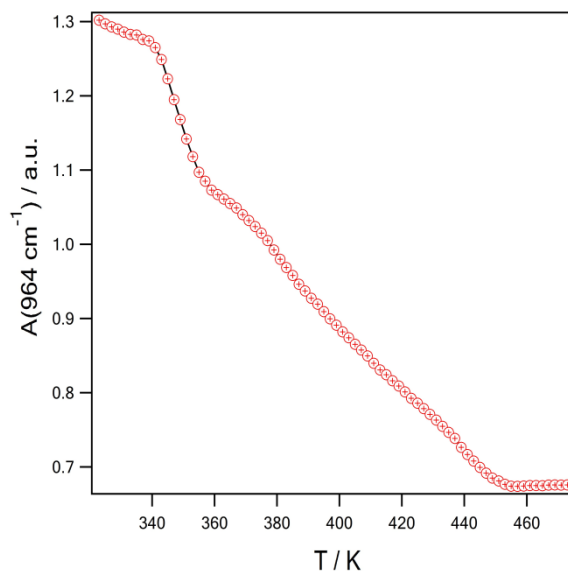
3 **Figure 4.** Temperature dependence of the absorption of the features due to the 18C6 crown for  
 4 examined compound: 1107  $\text{cm}^{-1}$  band (a); 964  $\text{cm}^{-1}$  band (b). Temperature dependence of the



- antisymmetric and symmetric  $\nu(\text{COO})$  peak position (c) and absorption of antisymmetric  $\nu(\text{COO})$
- band (d); absorptions of symmetric  $\nu(\text{COO})$  band (e).

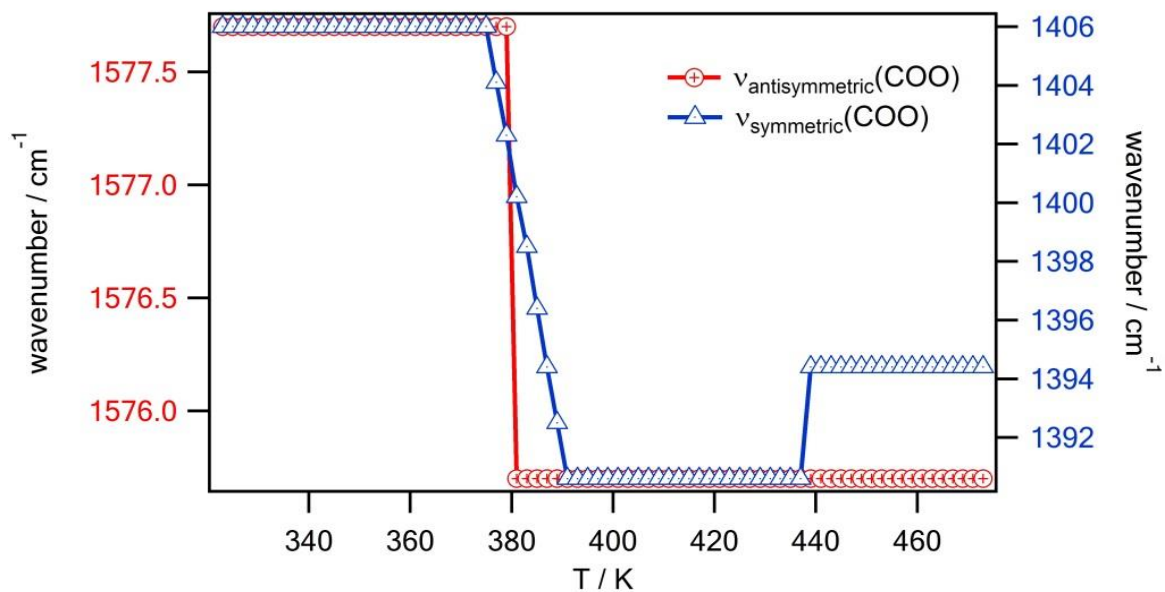


**a**

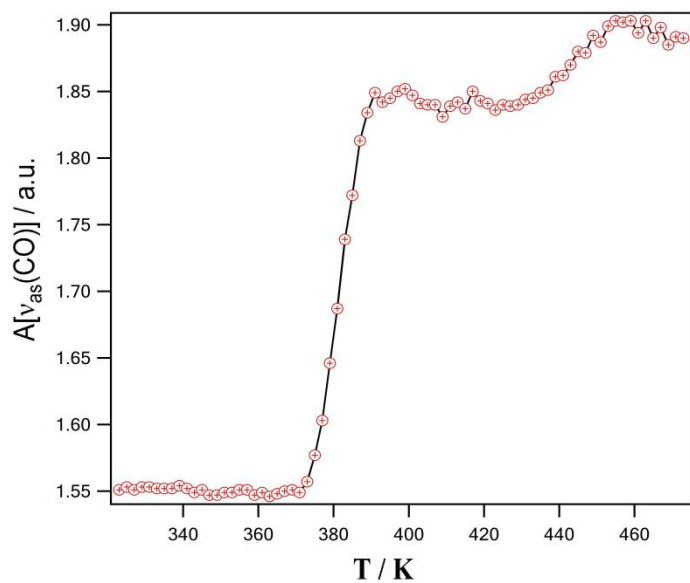


**b**

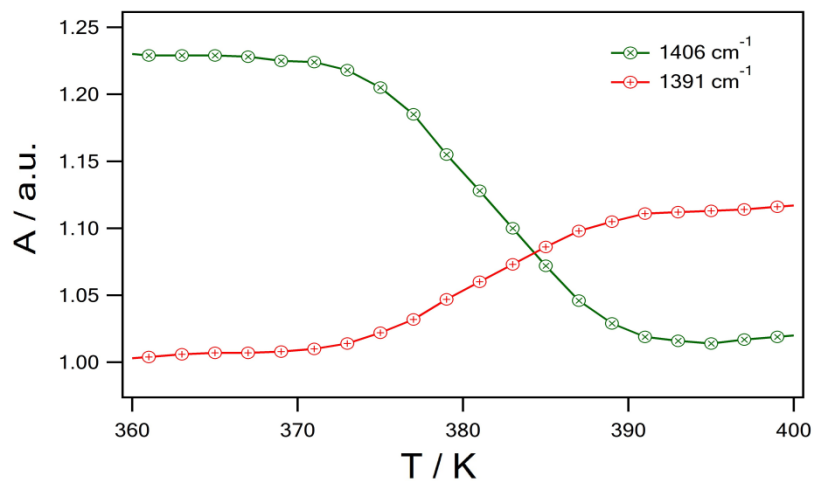
3



**c**



d



e

1

2

3 **Table 2.** Assignment of infrared spectra of the 18C6·NaCh complex at room temperature.

18C6·NaCh	Assignment
3457	water
3405	18C6
3289	unspecified $\nu(\text{CH})$
2972	unspecified $\nu(\text{CH})$
2938	unspecified $\nu(\text{CH})$

2913	18C6
2864	18C6
2824	18C6
1656	v(COO---H <sub>2</sub> O)
1578	antisymmetric v(COO)
1473	18C6
1432	18C6
1406	symmetric v(COO)
1351	18C6
1320	cholate
1292	18C6
1280	18C6
1268	cholate
1250	18C6
1227	unspecified alkyl
1205	cholate
1107	18C6
1082	unspecified alkyl
1045	cholate
985	cholate
965	18C6
837	18C6
785	
750	
712	
614	
590	18C6
528	18C6
475	18C6

---

1

2

3

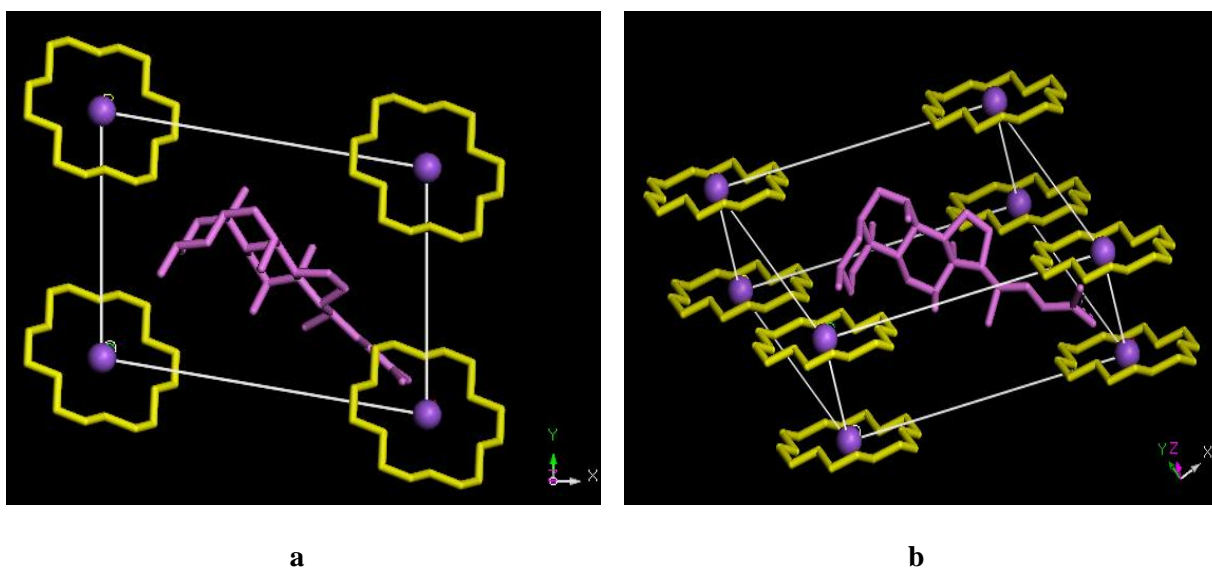
4

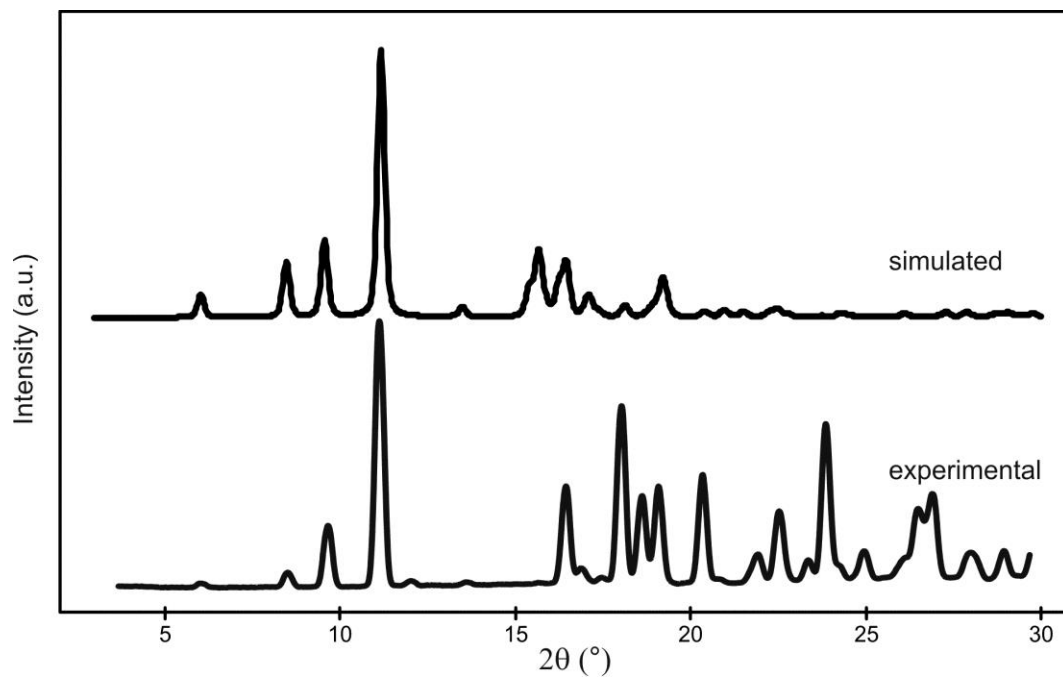
1 It is clear also from PXRD results (Figure 2d) that crystalline 18C6·NaCh complex suffers two  
2 phase changes, accompanied by dehydration. The RT phase (Figure 2d, Figure 5, Table 3) has been  
3 indexed to a triclinic lattice. It is already known that the cholic acid molecule crystallizes in  
4 orthorhombic system in a kind of crossing structure.<sup>58</sup> The intercalation of such molecule into the 18-  
5 crown-6 cavity, changes the type of crystal system, consequently causes the elongation of the *a* and *c*  
6 axes, and shortening of the *b* axis of the crystal lattice (Table 3). According to the results, complex  
7 exhibits two polymorphic transitions, both occurring simultaneously with dehydration of the sample, in  
8 accordance with other experimental results. The high temperature phases are monoclinic, as shown in  
9 Figure 6 and 7. As evident from Table 3, lattice parameters of the two monoclinic phases are very  
10 close to each other, suggesting that very similar structure. According to the quantum chemistry  
11 studies, this could be due to the changes of minimum energy 18C6-Na<sup>+</sup> conformers.<sup>4</sup>

12

13 **Figure 5.** Molecular model of the room temperature phase of 18C6·NaCh; view along *c*-axis, (a) side  
14 view (b). The 18-crowns are colored yellow, while the cholic group is colored purple. For clarity the  
15 hydrogen atoms are omitted. Experimental and simulated diffraction patterns of the room temperature  
16 phase of 18C6·NaCh (c).

17





c

1

2

3 **Table 3.** Lattice parameters of room temperature phase and higher temperature phases of 18C6·NaCh,  
 4 determined by PXRD.

<i>T</i> / K	structure type	lattice parameters						
		<i>a</i> / Å	<i>b</i> / Å	<i>c</i> / Å	$\alpha$ / °	$\beta$ / °	$\gamma$ / °	<i>V</i> / Å <sup>3</sup>
273	triclinic, <i>P</i> 1	15.45	10.60	6.84	91.7	105.6	98.6	1063.9
363	monoclinic, <i>P</i> 2	12.25	12.65	8.26	90.0	90.0	107.9	1218.0
390	monoclinic, <i>P</i> 2	12.16	11.60	8.20	90.0	90.0	103.0	1127.0

5

6

7

8

1           In order to construct the structural models of the three phases, diffraction patterns for proposed  
2 models were simulated and compared to those obtained by experiment. Figures 5, 6 and 7 show the  
3 models for which the best fit between simulated and experimental diffractograms has been achieved.  
4 PXRD diffractograms of 18C6·NaCh at different temperatures, as well as indexing of room  
5 temperature phase and higher temperature phases of 18C6·NaCh are shown in Figure S3 and Table S1  
6 in the Supporting Informations section. Having in mind the molecular mass of 18C6·NaCh, and  
7 assuming a density of  $1.0 \text{ g cm}^{-3}$ , the volume of the molecule can be estimated to be  $1155 \text{ \AA}^3$ .  
8 Comparison of this with unit cell volume suggests for all three phases that there is only one molecule  
9 is the unit cell. As the molecule is chiral, no mirror or inverse centre is possible in the structures. Thus,  
10 the space group of the triclinic phase can only be *P1* (Figure 5), as it was obtained also for 18C6-  
11 potassium picrate complex.<sup>52</sup> Formation of different host frameworks and network patterns within  
12 cholic acid compounds<sup>39–43</sup> seems to be very common. Cholic acid and *n*-alkylammonia form bilayer  
13 like structures in the monoclinic phase, sandwich-type structure for 1:1 complexes, and crossing-type  
14 bilayers for 2:1 complexes.<sup>42</sup> It seems that in this case, the arrangement in the triclinic phase also  
15 appears as layer like, with crown ether unit and sodium on one side, and the cholate anion on the other  
16 side, similar as found for 18C6-sodium 4-(1-pentylheptyl)benzenesulfonate.<sup>56</sup> Unlike these results, the  
17 crystal smectic phase layers of 18C6-sodium *n*-dodecylsulfate are composed of repetitive units of two  
18 crown ether layers with extended dodecyl chains.<sup>56</sup> For the two monoclinic phases (Figure 6 and 7),  
19 the fact that there exists a unique axis requires it being a 2-fold axis, so the space group can only be  
20 assigned as *P2*. In addition, as there is only one molecule in the unit cell and the molecule itself do not  
21 have a 2-fold rotational axis, we propose that the 2-fold symmetry originate from the molecules taking  
22 randomly one of the two different configurations, so called “orientational disorder” (related by a 2-  
23 fold symmetry) in the unit cell. This may also explain the diffuse scattering observed around  $2\theta = 22^\circ$   
24 for the two monoclinic phases.

25

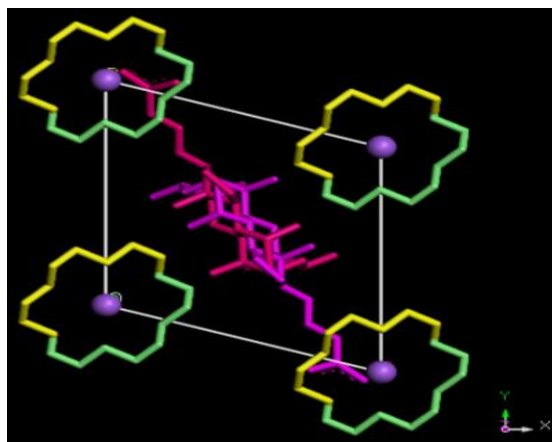
26

27

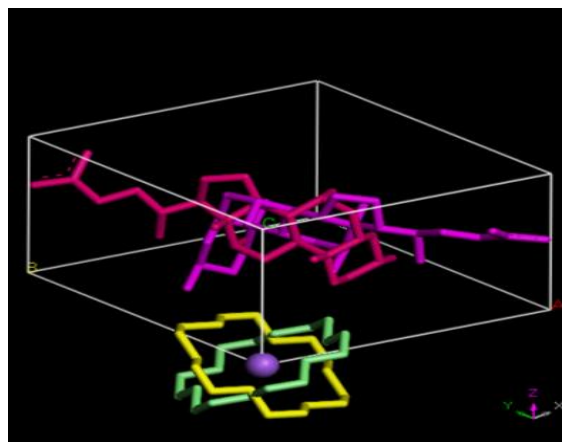
1 **Figure 6.** Molecular model of the medium temperature phase of 18C6·NaCh at 363 K: view along *c*-axis (a), side view (b, c). The 18-crowns are colored  
2 yellow and green, while the cholic group is colored purple and magenta. For clarity hydrogen atoms are omitted. The model before the application of the 2-  
3 fold rotational symmetry along *c*-axis (c). Experimental and simulated diffraction patterns of 18C6·NaCh at 363 K (d).

4

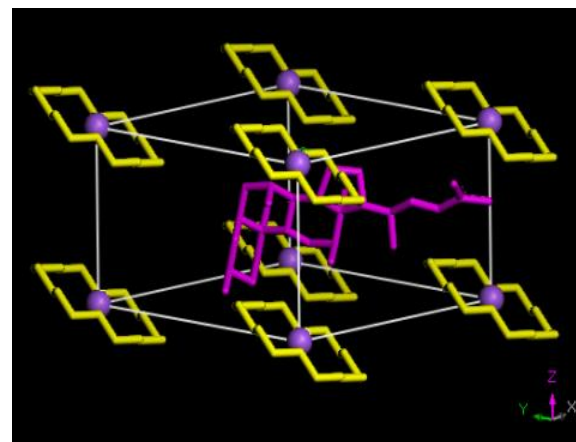
5



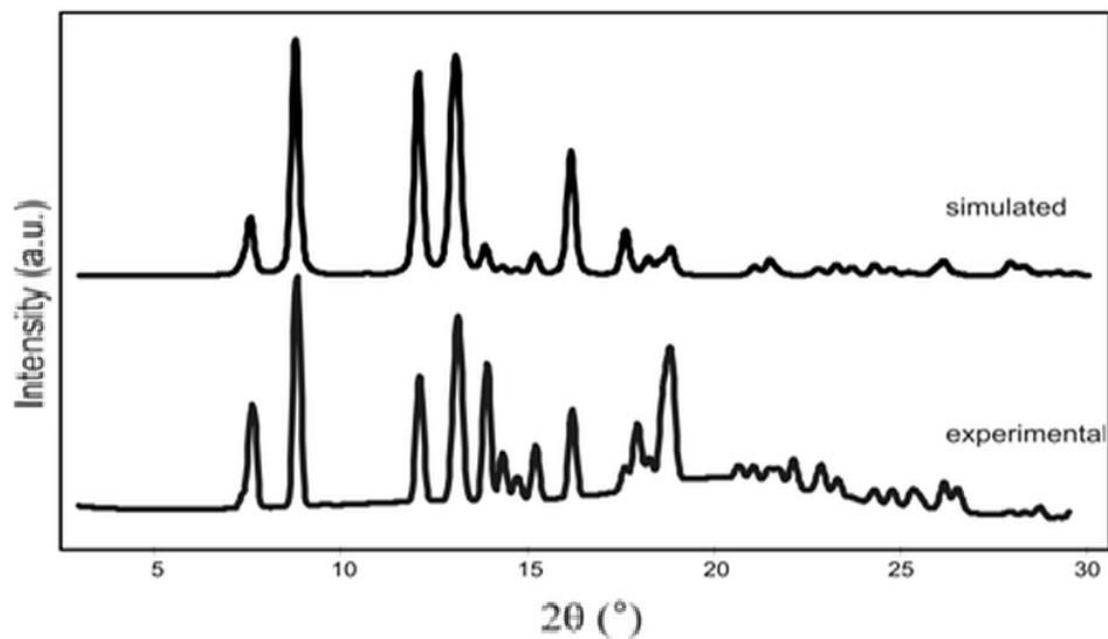
a



b



c



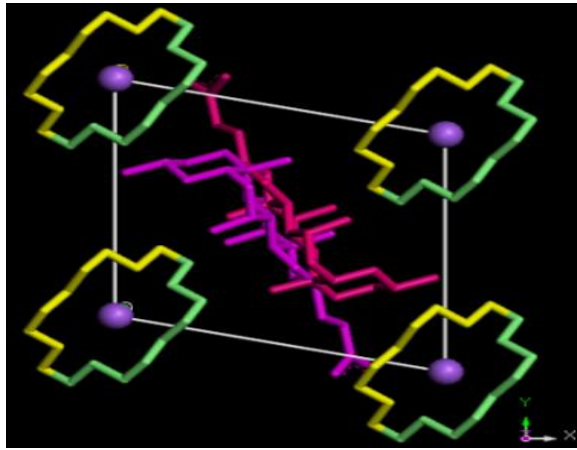
d

1

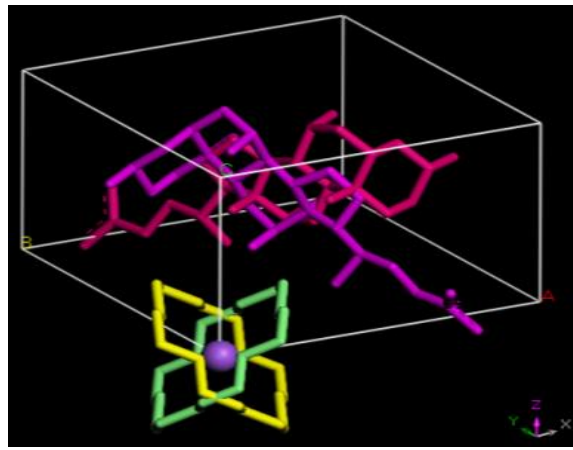
2

3 **Figure 7.** Molecular model of the high temperature phase of 18C6·NaCh at 390 K: view along *c*-axis (a) and side view (b, c). The 18-crowns are colored  
 4 yellow and green, while the cholic group is colored purple and magenta. For clarity hydrogen atoms are omitted. Only the model before the application of the  
 5 2-fold rotational symmetry along *c*-axis is shown in (c). Experimental and simulated diffraction patterns of 18C6·NaCh at 390 K (d).

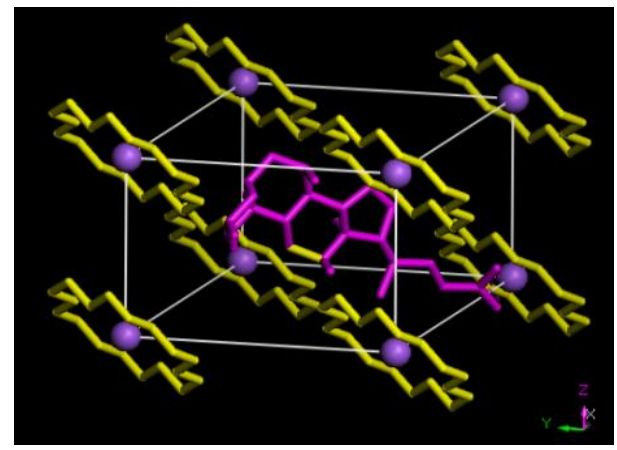




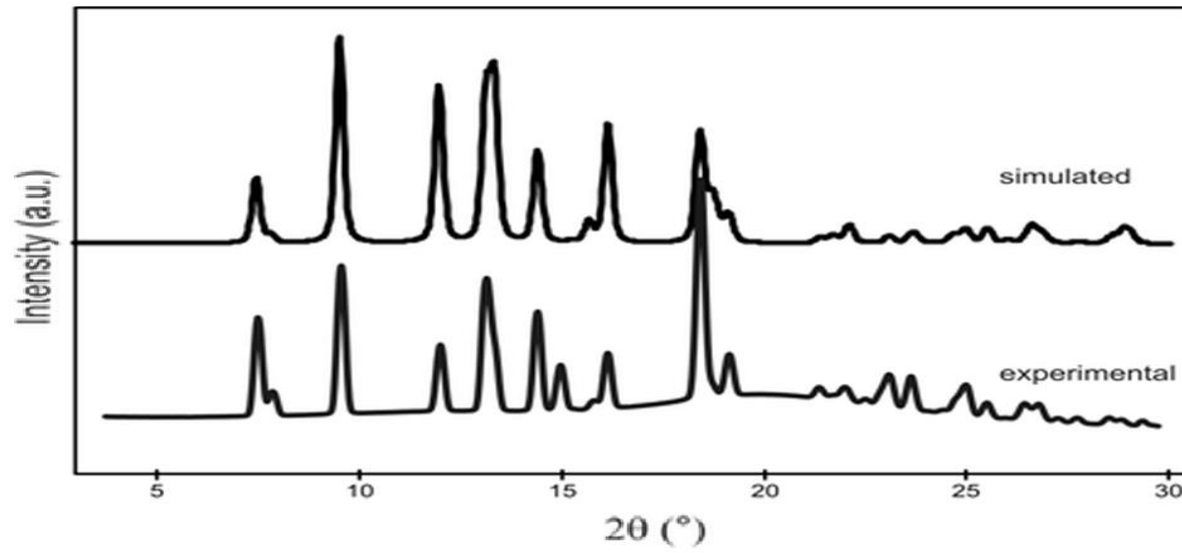
a



b



c



d

## 1 **Liquid-like state phase transitions**

2 Thermogravimetric analysis (Figure 2a) shows that the most prominent decrease in mass for  
3 this system occurs between 423 and 523 K, with the transition temperature (inflection point of TG for  
4 the mass decrease in the defined temperature period) of 493 K. The decrease in mass of the sample in  
5 the considered step with respect to starting mass  $m_0$  was 0.37, which is undoubtedly attributed to  
6 decomplexation with consequent evaporation of free 18C6 from sample. The transition temperatures  
7 and thermodynamic parameters given by the DSC together with the thermodynamic parameters for  
8 decomplexation, calculated from the absorbance measurement of complexed and decomplexed sodium  
9 salt (IR), explained in section 2.3, are shown in Table 1. Temperature-dependent infrared spectroscopy  
10 was used in order to explain the thermal changes on the molecular level for this temperature period  
11 (Figures 1c, 3 and 4).

12 IR spectra on Figure 4e shows isosbestic point at  $1395\text{ cm}^{-1}$ , which indicates simple  
13 equilibrium between NaCh·18C6 complex and NaCh. Above 400 K, area of  $\nu(\text{OH})$  region remains  
14 constant, reflecting that the sample is completely dehydrated and the absorbance in this region is  
15 exclusively due to the cholate OH groups. Microscopic observations detected at 400 K characteristic  
16 patterns of chiral nematic (cholesteric) – partly homeotropic, partly  $s = 1$  disclinations, with dark  
17 patches that indicate helix, *i.e.* chirality (Figure 1d), but the texture starts to disappear due to partial  
18 decomposition, which is in accordance with previously mentioned IR results. Thermal properties of  
19 18C6·NaCh complex are very similar to those obtained for 18C6-sodium *n*-dodecylsulfate and 18C6-  
20 sodium 4-(1-pentylheptyl)benzenesulfonate.<sup>56</sup> The formation of liquid crystalline phases is very  
21 common in complexes with crown ethers, but unlike the examined one, most of the mesophases  
22 formed are stable until isotropisation and are enantiotropic.<sup>45-51</sup> Unlike chiral nematic behavior noticed  
23 in the examined complex, smectic phases were obtained for other 18C6 complexes,<sup>56</sup> hexagonal  
24 columnar mesophases are formed in gallic acid substituted *ortho*-terphenyl dimers linked by a central  
25 18C6 ether<sup>40</sup> or dibenzo 18C6 with different alkyl chain lengths,<sup>46</sup> and nematic liquid crystals as well  
26 as smectic A phase in combination of 18C6 or rodlike 4,4'' didecyloxyp-terphenyl unit.<sup>56</sup> The diversity

1 in thermal and thermotropic behavior of 18C6 complexes points to the promoting effect of the  
2 attached groups or guest molecules in the complex.

3         The partial decomposition also matches with the result of temperature dependence of the IR  
4 baseline absorption at  $2500\text{ cm}^{-1}$ , shown in Figure 3c. The slow decomplexation is seen as an abrupt  
5 increase of absorbance above 395 K, with a transition temperature at 445 K, as determined by  
6 differentiation. In this range, a simultaneous decrease of the absorption at 1107, 964 and  $837\text{ cm}^{-1}$   
7 (Figure 4a and b) indicates the release of 18C6 from the sample. However, it should be mentioned that  
8 IR baseline behave different to TG, indicating significantly lower transition temperatures. However,  
9 this is not surprising, since the two techniques reflect different processes. Namely, the variation of IR  
10 baseline absorption is due to decomplexation of the 18C6 from  $\text{Na}^+$ . On the other hand, TG reflects  
11 evaporation of the free 18C6 from the sample. Intensity of IR features due to 18C6 vibrations are  
12 much better correlated with TG.

13         A steeper drop of the intensities of all IR spectral features due to the 18C6 moiety above 410  
14 K is well correlated with TG, and is explained by evaporation of free crown 18C6 from the sample,  
15 which is now of liquid-like appearance. The difference in the shapes of curves is a result of the  
16 different oscillators, which cause these bands. The band at  $1107\text{ cm}^{-1}$  is due to the  $\nu(\text{C-O})$  of crown  
17 ether. Thus, the change in absorption occurs due both to decomplexation and diffusion, resulting in  
18 nonlinear dependence. On the other hand, the band at  $964\text{ cm}^{-1}$  is assigned to  $\nu(\text{C-O-C})$  and is only  
19 slightly affected by complexation. Thus, its decrease reflects only diffusion of crown 18C6 from the  
20 system, resulting in linear dependence. Obviously, diffusion in the liquid phase is significantly  
21 facilitated by transition to liquid phase. After that, a moderate change in the symmetric band position,  
22 accompanied by increase of both symmetric and antisymmetric  $\nu(\text{COO})$  band intensity occurs at 440  
23 K, which coincides to transition between liquid crystal to disordered liquid phase (isotropisation) with  
24 simultaneous but complete decomposition (Table 1).

25

26

#### 1 4. CONCLUSIONS

2 Compound constituting of 18C6 ether and NaCh surfactant was synthesized as 1:1  
3 coordination complex, and its structure was confirmed with elemental analysis and NMR  
4 spectroscopy. Its thermal behavior was examined by the techniques that were of great  
5 complementarity. Thermogravimetric and differential thermal analysis, differential scanning  
6 calorimetry, temperature-dependent IR spectroscopy, PXRD and microscopic observations gave a  
7 detailed insight about phase transitions of the complex. Temperature dependent IR spectroscopy and  
8 PXRD solved the problem on the molecular level and gave a detailed view of the microscopic  
9 background of macroscopically observable phase transitions. The structure during thermal treatment  
10 was observed with powder XRD, and molecular models of the phases are made. Very good fit is  
11 achieved between the experimental and calculated values of the diffraction angles and the molecular  
12 models presented are results of tedious trial-and-error work to get intensity matching. Considering the  
13 low symmetry (triclinic and monoclinic) and powder diffraction, this gave very valuable informations  
14 on the changes of ordering during the solid-state phase transitions.

15 18C6·NaCh complex shows complex thermal behavior. Dehydration of the sample is a two-  
16 step process, occurring at 350 and 380 K. The two water molecules are absorbed to each formula unit,  
17 where the first is hydrogen bonded to 18C6 ligand and another to carboxylic group of cholate anion.  
18 Complex goes through two solid-solid polymorphic transitions, accompanied with dehydration. The  
19 room temperature phase is indexed to a triclinic lattice with the *P1* space group, while the high  
20 temperature phases are monoclinic with the *P2* space group, and there is only 1 molecule in the unit  
21 cell. The lattice parameters of the two monoclinic phases are very similar to each other, suggesting  
22 that their structure is also very similar. The molecules take randomly one of the two different  
23 configurations in the unit cell, resulting in the 2-fold symmetry.

24 The formation of liquid crystalline phase seen through characteristic patterns of cholesteric  
25 phase occurs simultaneously with partial decomposition. This process is followed by the complete  
26 decomplexation of the Na<sup>+</sup> ion from crown 18C6 ligand and consequent diffusion of crown 18C6 from  
27 the sample, seen as an abrupt increase of absorbance in the IR spectra above 395 K, with a transition

1 temperature at 445 K. The study provides the relationship between molecular structure, thermal  
2 properties, and stability of the complex. We hope this work will be useful for the previously  
3 mentioned potential applications of this new, and similar synthesized crown complexes.

4

5

6

7

8

9

10

11

12

13

14

15

16

17

18

19

20

21

1 **Acknowledgment.**

2 This work has received support from the Ministry of Education, Science and Sport of the  
3 Republic of Croatia (Projects No. 098-0982915-2949, 098-0982904-2927, 098-0982904-2941).  
4 Authors are grateful to prof. dr. sc. G. Ungar and dr. sc. Xiangbing Zeng, Department of Materials  
5 Science and Engineering, University of Sheffield, for the PXRD measurements and interpretation of  
6 the obtained diffractograms.

7  
8 **Supporting Information Available.**

9 This material is available free of charge via the Internet at <http://pubs.acs.org>.

10

11

12

13

14

15

16

17

18

19

20

21

22

23

24

## 1 **References**

- 2 (1) Gámez, F.; Hurtado, P.; Martínez-Haya, B.; Berden, G.; Oomens, J. Vibrational Study of  
3 Isolated 18-Crown-6 Ether Complexes with Alkaline-Earth Metal Cations. *Int. J. Mass*  
4 *spectrom.* **2011**, *308*, 217–224.
- 5 (2) Izatt, R. M.; Pawlak, K.; Bradshaw, J. S.; Bruening, R. L. Thermodynamic and Kinetic Data for  
6 Macrocycle Interactions with Cations and Anions. *Chem. Rev.* **1991**, *91*, 1721–2085.
- 7 (3) Markova, N. V.; Vasiliev, V. P. Thermochemistry of 18C6 Complexation with Alkali, Alkaline  
8 Earth Metal Cations and Ammonium Ion. *J. Therm. Anal.* **1995**, *45*, 695–701.
- 9 (4) De, S. Preferential Interaction of Charged Alkali Metal Ions (guest) within a Narrow Cavity of  
10 Cyclic Crown Ethers (neutral Host): A Quantum Chemical Investigation. *J. Mol. Struct.* **2010**,  
11 *941*, 90–101.
- 12 (5) Anderson, J.; Paulsen, E. S.; Dearden, D. V. Alkali Metal Binding Energies of Dibenzo-18-  
13 Crown-6: Experimental and Computational Results. *Int. J. Mass spectrom.* **2003**, *227*, 63–76.
- 14 (6) Doxsee K.M.; Francis P.E.; Weakley T.J.R. Hydration, Ion Pairing, and Sandwich Motifs in  
15 Ammonium Nitrate Complexes of Crown Ethers. *Tetrahedron* **2000**, *56*, 6683–6691.
- 16 (7) Hurtado, P.; Hortal, A. R.; Gámez, F.; Hamad, S.; Martínez-Haya, B. Gas-Phase Complexes of  
17 Cyclic and Linear Polyethers with Alkali Cations. *Phys. Chem. Chem. Phys.* **2010**, *12*, 13752–  
18 13758.
- 19 (8) Martínez-Haya, B.; Hurtado, P.; Hortal, A. R.; Hamad, S.; D. Steill, J.; Oomens, J. Emergence  
20 of Symmetry and Chirality in Crown Ether Complexes with Alkali Metal Cations. *J. Phys.*  
21 *Chem. A* **2010**, *114*, 7048–7054.
- 22 (9) Peiris, D. M.; Yang, Y.; Ramanathan, R.; Williams, K. R.; Watson, C. H.; Eyler, J. R. Infrared  
23 Multiphoton Dissociation of Electrosprayed Crown Ether Complexes. *Int. J. Mass Spect. Ion*  
24 *Proc.* **1996**, *157–158*, 365–378.
- 25 (10) Pedersen, C. J. Cyclic Polyethers and Their Complexes with Metal Salts. *J. Am. Chem. Soc.*  
26 **1967**, *89*, 7017–7036.

- 1 (11) Raevsky, O. A.; Solov'ev, V. P.; Solotnov, A. F.; Schneider, H.-J.; Rüdiger, V. Conformation  
2 of 18-Crown-5 and Its Influence on Complexation with Alkali and Ammonium Cations: Why  
3 18-Crown-5 Binds More Than 1000 Times Weaker Than 18C6. *J. Org. Chem.* **1996**, *61*, 8113–  
4 8116.
- 5 (12) Cram, D. Synthetic Host-Guest Chemistry. In *Applications of Biochemical Systems in Organic*  
6 *Chemistry*; Wiley: New York, NY, USA, 1976; Vol. 10, p. 815.
- 7 (13) Vögtle, F.; Weber, E. *Host Guest Complex Chemistry: Macrocycles : Synthesis, Structures,*  
8 *Applications*; Springer, 1985.
- 9 (14) Unruh, G.; Cumbest, J. Crown Ethers Enhance Ionic Residue Removal. *Res. Develop.* **1994**.
- 10 (15) Moyer, B. A.; Birdwell, J. F.; Bonnesen, P. V.; Delmau, L. H. Use of Macrocycles in Nuclear-  
11 Waste Cleanup: A Realworld Application of a Calixcrown in Cesium Separation Technology.  
12 In *Macrocyclic Chemistry*; Gloe, K., Ed.; Springer-Verlag: Berlin/Heidelberg; pp. 383–405.
- 13 (16) Darwish, I. A.; Uchegbu, I. F. The Evaluation of Crown Ether Based Niosomes as Cation  
14 Containing and Cation Sensitive Drug Delivery Systems. *Int. J. Pharm.* **1997**, *159*, 207–213.
- 15 (17) Muzzalupo, R.; Nicoletta, F. P.; Trombino, S.; Cassano, R.; Iemma, F.; Picci, N. A New Crown  
16 Ether as Vesicular Carrier for 5-Fluoruracil: Synthesis, Characterization and Drug Delivery  
17 Evaluation. *Colloids Surf. B* **2007**, *58*, 197–202.
- 18 (18) Gokel, G. W.; Durst, H. D. Crown Ether Chemistry: Principles and Applications.  
19 *Aldrichim. Acta* **1976**, *9*, 3–12.
- 20 (19) Bereczki, R.; Ágai, B.; Bitter, I. Synthesis and Alkali Cation Extraction Ability of New Mono  
21 and Bis(benzocrown Ether)s with Terminal Alkenyl Groups. *J. Inclusion Phenom.* **2003**, *47*,  
22 53–58.
- 23 (20) Nakajima, M.; Kimura, K.; Shono, T. Liquid Chromatography of Alkali and Alkaline Earth  
24 Metal Salts on Poly(benzo-15-Crown-5)- and Bis(benzo-15-Crown-5)-Modified Silicas. *Anal.*  
25 *Chem.* **1983**, *55*, 463–467.
- 26 (21) Jin, Y.; Fu, R.; Huang, Z. Use of Crown Ethers in Gas Chromatography. *J. Chromatogr. A*  
27 **1989**, *469*, 153–159.



- 1 (22) Wong, A.; Wu, G. Solid-State  $^{23}\text{Na}$  Nuclear Magnetic Resonance of Sodium Complexes with  
2 Crown Ethers, Cryptands, and Naturally Occurring Antibiotic Ionophores: A Direct Probe to  
3 the Sodium-Binding Sites. *J. Phys. Chem. A* **2000**, *104*, 11844–11852.
- 4 (23) Koch, K. J.; Aggerholm, T.; Nanita, S. C.; Cooks, R. G. Clustering of Nucleobases with Alkali  
5 Metals Studied by Electrospray Ionization Tandem Mass Spectrometry: Implications for  
6 Mechanisms of Multistrand DNA Stabilization. *J. Mass Spectrom.* **2002**, *37*, 676–686.
- 7 (24) Chaput, J. C.; Switzer, C. A DNA Pentaplex Incorporating Nucleobase Quintets. *Proceedings*  
8 *Nat. Ac. Sci.* **1999**, *96*, 10614–10619.
- 9 (25) Kudo, Y.; Katsuta, S.; Takeda, Y. Potentiometric Determination of the Ion-Pair Formation  
10 Constant of a Univalent Cation-Neutral Ligand Complex with an Anion in Water Using an Ion-  
11 Selective Electrode. *Anal. Sci.* **1999**, *15*, 597–599.
- 12 (26) Hofmann, A. F. Bile Acids as Drugs: Principles, Mechanisms of Action and Formulations. *Ital*  
13 *J Gastroenterol.* **1995**, *27*, 106–113.
- 14 (27) Berlati, F.; Ceschel, G.; Clerici, C.; Pellicciari, R.; Roda, A.; Ronchi, C. The Use of Bile  
15 Acids as Antiviral Agents. WO 9400126 1994.
- 16 (28) Marples, B.; Stretton, R. Use of Steroidal Compounds as Anti-Fungal Agents. WO 9013298.
- 17 (29) Savage, P. B.; Li, C.; Taotafa, U.; Ding, B.; Guan, Q. Antibacterial Properties of Cationic  
18 Steroid Antibiotics. *FEMS Microbiol. Lett.* **2002**, *217*, 1–7.
- 19 (30) Davis, A. P.; Joos, J.-B. Steroids as Organising Elements in Anion Receptors. *Coord. Chem.*  
20 *Rev.* **2003**, *240*, 143–156.
- 21 (31) Nath, S.; Maitra, U. A Simple and General Strategy for the Design of Fluorescent Cation  
22 Sensor Beads. *Org. Lett.* **2006**, *8*, 3239–3242.
- 23 (32) Soto Tellini, V. H.; Jover, A.; Meijide, F.; Vázquez Tato, J.; Galantini, L.; Pavel, N. V.  
24 Supramolecular Structures Generated by a P-Tert-Butylphenyl-Amide Derivative of Cholic  
25 Acid: From Vesicles to Molecular Tubes. *Advan. Mater.* **2007**, *19*, 1752–1756.
- 26 (33) Yoshii, M.; Yamamura, M.; Satake, A.; Kobuke, Y. Supramolecular Ion Channels from a  
27 Transmembrane Bischolic Acid Derivative Showing Two Discrete Conductances. *Org. Biomol.*  
28 *Chem.* **2004**, *2*, 2619–2623.

- 1 (34) Judd, L. W.; Davis, A. P. From Cholapod to Cholaphane Transmembrane Anion Carriers:  
2 Accelerated Transport through Binding Site Enclosure. *Chem. Comm.* **2010**, *46*, 2227–2229.
- 3 (35) Bonar-Law, R. P.; Mackay, L. G.; Sanders, J. K. M. Morphine Recognition by a Porphyrin–  
4 cyclocholeate Molecular Bowl. *J. Chem. Soc., Chem. Commun.* **1993**, 456–458.
- 5 (36) Balasubramanian, R.; Maitra, U. Design and Synthesis of Novel Chiral Dendritic Species  
6 Derived from Bile Acids. *J. Org. Chem.* **2001**, *66*, 3035–3040.
- 7 (37) Maitra, U.; Balasubramanian, S. Design and Synthesis of New Bile Acid-Based Macrocycles.  
8 *J. Chem. Soc., Perkin Trans. 1* **1995**, 83–88.
- 9 (38) Nakano, K.; Mochizuki, E.; Yasui, N.; Morioka, K.; Yamauchi, Y.; Kanehisa, N.; Kai, Y.;  
10 Yoswathananont, N.; Tohnai, N.; Sada, K.; et al. Mechanism of Selective and Unselective  
11 Enclathration by a Host Compound Possessing Open, Flexible Host Frameworks. *European J.*  
12 *Org. Chem.* **2003**, *2003*, 2428–2436.
- 13 (39) Nakano, K.; Sada, K.; Kurozumi, Y.; Miyata, M. Importance of Packing Coefficients of Host  
14 Cavities in the Isomerization of Open Host Frameworks: Guest-Size-Dependent Isomerization  
15 in Cholic Acid Inclusion Crystals with Monosubstituted Benzenes. *Chem. Eur. J.* **2001**, *7*, 209–  
16 220.
- 17 (40) Miyata, M.; Sada, K. Deoxycholic Acid and Related Hosts. In *Comprehensive Supramolecular*  
18 *Chemistry*; Atwood, J. L.; Davies, J.; McNicol, D.; Lehn, J.; Toda, F.; Bishop, R., Eds.;  
19 Pergamon: Oxford, 1966; Vol. 6, pp. 147–176.
- 20 (41) Valkonen, A.; Lahtinen, M.; Tamminen, J.; Kolehmainen, E. Solid State Structural Studies of  
21 Five Bile Acid Derivatives. *J. Mol. Struct.* **2008**, *886*, 197–206.
- 22 (42) Tomašić, V.; Štefanić, Z. Cholic Acid as Host for Long Linear Molecules: A Series of Co-  
23 Crystals with N-Alkylammonia. *Cryst. Eng. Comm.* **2007**, *9*, 1124–1128.
- 24 (43) Miyata, M.; Tohnai, N.; Hisaki, I. Supramolecular Chirality in Crystalline Assemblies of Bile  
25 Acids and Their Derivatives; Three-Axial, Tilt, Helical, and Bundle Chirality. *Molecules* **2007**,  
26 *12*, 1973–2000.

- 1 (44) Kato, K.; Tohnai, N.; Miyata, M. Hierarchical Prediction Process of Cholic Acid Crystal  
2 Structures Based on Characteristic Helical Assemblies. *Mol. Cryst. Liq. Cryst.* **2005**, *440*, 125–  
3 132.
- 4 (45) Steinke, N.; Kaller, M.; Nimtz, M.; Baro, A.; Laschat, S. Columnar Liquid Crystals Derived  
5 from Crown Ethers with Two Lateral Ester-Substituted Ortho-Terphenyl Units: Unexpected  
6 Destabilisation of the Mesophase by Potassium Iodide. *Liq. Cryst.* **2010**, *37*, 1139–1149.
- 7 (46) Schultz, A.; Laschat, S.; Saipa, A.; Gießelmann, F.; Nimtz, M.; Schulte, J. L.; Baro, A.;  
8 Miehl, B. Columnar Liquid Crystals with a Central Crown Ether Unit. *Adv. Funct. Mater.*  
9 **2004**, *14*, 163–168.
- 10 (47) Nagvekar, D. S.; Delaviz, Y.; Prasad, A.; Merola, J. S.; Marand, H.; Gibson, H. W. Synthesis  
11 and Properties of Cholesteryl Esters Bearing 32- and 16-Membered Crown Ethers. *J. Org.*  
12 *Chem.* **1996**, *61*, 1211–1218.
- 13 (48) Goodby, J.; Mehl, G.; Saez, I.; Tuffin, R.; Mackenzie, G.; Auzely-velty, R.; Benvegna, T.;  
14 Plusquellec, D. Liquid Crystals with Restricted Molecular Topologies: Supermolecules and  
15 Supramolecular Assemblies. *Chem. Inform.* **1998**, *29*, 2057–2070.
- 16 (49) Leblanc, K.; Berdagué, P.; Rault, J.; Bayle, J.-P.; Judeinstein, P. Synthesis and Ionic Properties  
17 of Nematic Compounds Bearing an Ether-Crown Moiety: An NMR Approach. *Chem.*  
18 *Commun.* **2000**, 1291–1292.
- 19 (50) Nishikawa, Y.; Watanabe, T.; Yoshida, H.; Ikeda, M. Phase Transition Behaviors of Crown-  
20 Ether Derivative and Its Sodium Ion Complex. *Thermochim. Acta* **2005**, *431*, 81–86.
- 21 (51) He, G. X.; Wada, F.; Kikukawa, K.; Shinkai, S.; Matsuda, T. Syntheses and Thermal Properties  
22 of New Liquid Crystals Bearing a Crown Ether Ring: Cation Binding in the Nematic Phase. *J.*  
23 *Org. Chem.* **1990**, *55*, 541–548.
- 24 (52) Barnes, J.; Collard, J. 18-Crown-6–potassium Picrate (1/1). *Acta Crystallogr., Sect. C: Cryst.*  
25 *Struct. Commun.* **1988**, *44*, 565–566.
- 26 (53) Ahonen, K. V.; Lahtinen, M. K.; Löfman, M. S.; Kiesilä, A. M.; Valkonen, A. M.; Sievänen, E.  
27 I.; Nonappa; Kolehmainen, E. T. Structural Studies of Five Novel Bile Acid-4-Aminopyridine  
28 Conjugates. *Steroids* **2012**, *77*, 1141–1151.

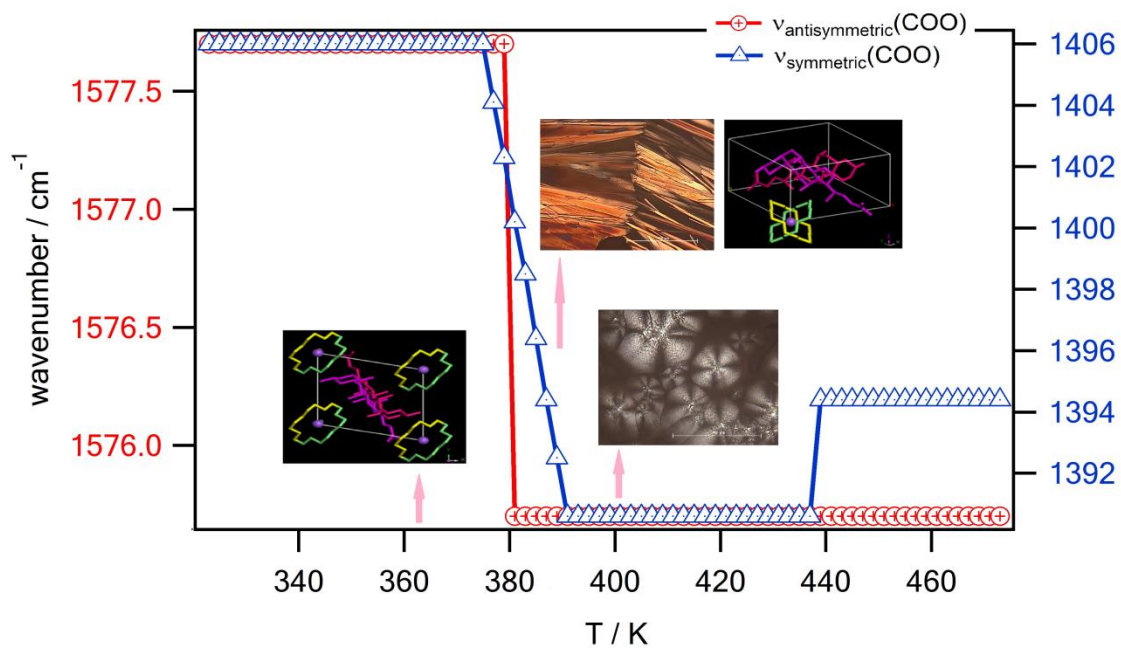
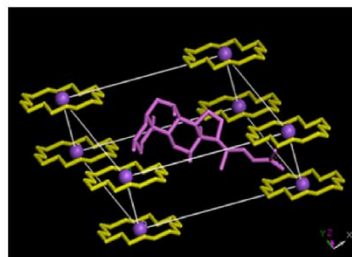
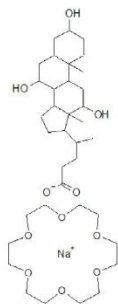
- 1 (54) Mejjide, F.; Trillo, J. V.; Frutos, S. de; Galantini, L.; Pavel, N. V.; Soto, V. H.; Jover, A.; Tato,  
2 J. V. Crystal Structure of Head-to-Head Dimers of Cholic and Deoxycholic Acid Derivatives  
3 with Different Symmetric Bridges. *Steroids* **2013**, *78*, 247–254.
- 4 (55) Zimmermann, B.; Baranović, G. Determination of Phase Transition Temperatures by the  
5 Analysis of Baseline Variations in Transmittance Infrared Spectroscopy. *Appl. Spectrosc.* **2009**,  
6 *63*, 1152–1161.
- 7 (56) Mihelj, T.; Tomašić, V.; Biliškov, N.; Liu, F. Temperature-Dependent IR Spectroscopic and  
8 Structural Study of 18-Crown-6 Chelating Ligand in the Complexation with Sodium Surfactant  
9 Salts and Potassium Picrate. *Spectrochim. Acta A* **2014**, *124*, 12–20.
- 10 (57) Tomašić, V.; Biliškov, N.; Mihelj, T.; Štefanić, Z. Thermal Behaviour and Structural Properties  
11 of surfactant—Picrate Compounds: The Effect of the Ammonium Headgroup Number.  
12 *Thermochim. Acta* **2013**, *569*, 25–35.
- 13 (58) Miki, K.; Kasai, N.; Shibakami, M.; Chirachanchai, S.; Takemoto, K.; Miyata, M. Crystal  
14 Structure of Cholic Acid with No Guest Molecules. *Acta. Crystallogr. C* **1990**, *46*, 2442–2445.
- 15  
16  
17  
18  
19  
20  
21  
22  
23  
24  
25

1 Table of Contents Graphic

2 18-crown-6-sodium cholate complex: thermochemistry, structure and stability

3 Tea Mihelj, Vlasta Tomašić, Nikola Biliškov

4



5

6

7

8